

Tunable phonon-photon coupling induces double magnomechanically induced transparency and enhances slow light in an atom-opto-magnomechanical system

M'bark Amghar, Noura Chabar, and Mohamed Amazioug

Citation: Chin. Phys. B, 2024, 33 (**12**): 120308. DOI: 10.1088/1674-1056/ad8cbb
Journal homepage: http://cpb.iphy.ac.cn; http://iopscience.iop.org/cpb

What follows is a list of articles you may be interested in

General multi-attack detection for continuous-variable quantum key distribution with local local oscillator

Zhuo Kang(康茁), Wei-Qi Liu(刘维琪), Jin Qi(齐锦), and Chen He(贺晨)
Chin. Phys. B, 2024, 33 (**5**): 050308. DOI: 10.1088/1674-1056/ad2bf2

Enhancing quantum temporal steering via frequency modulation

Mengkai Wu(吴孟凯) and Weiwen Cheng(程维文)
Chin. Phys. B, 2024, 33 (**5**): 050306. DOI: 10.1088/1674-1056/ad2505

Non-Gaussian approach: Withstanding loss and noise of multi-scattering underwater channel for continuous-variable quantum teleportation

Hao Wu(吴昊), Hang Zhang(张航), Yiwu Zhu(朱益武), Gaofeng Luo(罗高峰), Zhiyue Zuo(左峙岳), Xinchao Ruan(阮新朝), and Ying Guo(郭迎)
Chin. Phys. B, 2023, 32 (**10**): 100311. DOI: 10.1088/1674-1056/ace681

Floquet scattering through a parity-time symmetric oscillating potential

Xuzhen Cao(曹序桢), Zhaoxin Liang(梁兆新), and Ying Hu(胡颖)
Chin. Phys. B, 2023, 32 (**3**): 030302. DOI: 10.1088/1674-1056/aca39a

Fringe removal algorithms for atomic absorption images: A survey

Gaoyi Lei(雷高益), Chencheng Tang(唐陈成), and Yueyang Zhai(翟跃阳)
Chin. Phys. B, 2022, 31 (**5**): 050313. DOI: 10.1088/1674-1056/ac3758

Tunable phonon–photon coupling induces double magnomechanically induced transparency and enhances slow light in an atom-opto-magnomechanical system

M′bark Amghar[†], Noura Chabar, and Mohamed Amazioug[‡]

LPTHE, Department of Physics, Faculty of Sciences, Ibnou Zohr University, Agadir, Morocco

(Received 17 August 2024; revised manuscript received 20 October 2024; accepted manuscript online 30 October 2024)

We theoretically investigate the magnomechanically induced transparency phenomenon, Fano resonance and the slow–fast light effect in the situation where an atomic ensemble is placed inside the hybrid cavity of an opto-magnomechanical system. The system is driven by dual optical and phononic drives. We show double magnomechanically induced transparency in the probe output spectrum by exploiting the phonon–photon coupling strength. Then, we study the effects of the decay rate of the cavity and the atomic ensemble on magnomechanically induced transparency. In addition, we demonstrate that effective detuning of the cavity field frequency changes the transparency window from a symmetrical to an asymmetrical profile, resembling Fano resonances. Further, the fast and slow light effects in the system are explored. We show that the slow light profile is enhanced by adjusting the phonon–photon coupling strength. This result may have potential applications in quantum information processing and communication.

Keywords: cavity magnomechanics, magnomechanically induced transparency, Fano resonance, absorption, dispersion, transmission, slow light, fast light

PACS: 03.67.–a, 42.50.Gy, 42.50.Ex **DOI:** 10.1088/1674-1056/ad8cbb

1. Introduction

The interaction between light and matter has emerged as a dynamic and significant area of research, with broad potential applications across various domains. These applications include optomechanically induced transparency (OMIT),[1–6] coherent control of light,[7,8] electromagnetically induced transparency (EIT)[9–14] and the preparation of entanglement between cavity fields and macroscopic oscillators[15–24]. Recently, this research has played a pivotal role in advancing the field of solid quantum memory and quantum information processing. EIT is a common quantum interference effect observed in three-level atoms.[25] It describes the intriguing phenomenon whereby the absorption rate of atoms can be diminished to zero when they are exposed to an auxiliary laser field. This reduction is primarily a result of interference effects or dark state resonance in an excited state. Furthermore, analogous to EIT, when destructive interference occurs between the anti-Stokes scattering field and the weak probe field it is referred to as OMIT.[26] This phenomenon has been the subject of extensive research, both theoretically[1,2] and experimentally.[3,4] The multiple-OMIT phenomenon has been studied theoretically in a variety of innovative cavity optomechanical systems that have emerged in recent years, including hybrid piezo-optomechanical cavity systems,[27] atomic-media assisted optomechanical systems,[28] multiple-resonator optomechanical systems,[29] and so on. The complexity of light–matter interactions can also be seen in the phenomenon of Fano resonance, which is characterized by quantum interference between a discrete state and a continuum of states, producing asymmetric absorption profiles.[30] This phenomenon, first observed in atomic systems,[31] results in visible minima in the absorption spectrum.[32] Over the years, Fano resonance has been studied in various physical systems, such as optomechanical systems,[30,33] photonic crystals[34] and coupled micro-resonators.[35] Recently, experimental evidence of Fano-like asymmetric shapes has been reported in a hybrid cavity magnomechanical system.[36,37]

Cavity magnomechanics[37–40] has drawn more attention lately due to its potential for larger-scale quantum state preparation[41–43] and its numerous intriguing uses in quantum information science and technology.[44–50] It investigates interactions between microwave cavity photons, magnons (the collective excitation of a large number of spins) and vibratory phonons induced by magnetostriction in magnetically ordered materials such as yttrium iron garnet (YIG).[37–40,51–55] The combination of cavity optomechanics and cavity magnomechanics, obtained by coupling the magnomechanical displacement to an optical cavity via radiation pressure, creates the new system of opto-magnomechanics.[56–58] This hybrid system provides the capability to optically detect the population of magnons,[56] manipulate diverse magnonic quantum states within solid materials[57] and generate entanglement between optomagnonic[57] and microwave optics.[58] Consequently, this system holds great promise for applications in

[†]Corresponding author. E-mail: amghar.mbark98@gmail.com
[‡]Corresponding author. E-mail: amazioug@gmail.com

© 2024 Chinese Physical Society and IOP Publishing Ltd

quantum information processing and the development of quantum networks. Recently, magnomechanically induced transparency (MMIT) and slow–fast light have been studied in magnomechanical systems by modifying the strength of the atom–cavity coupling, without taking into consideration the cavity–phonon coupling.[59]

In this work, we propose and analyze the optomagnomechanically induced transparency phenomenon, Fano resonance and the fast–slow light effect within a cavity optomagnomechanical setup. This configuration includes optical cavity photons, magnons in a YIG crystal, magnetostriction-induced vibration phonons and an ensemble of two-level atoms (see Fig. 1). Magnon–phonon and phonon–photon interactions give rise to MMIT and OMIT in the probe output spectrum. Furthermore, we explore the impact of optomechanical coupling on the transmission and the phase spectra. We also study the influence of the decay rates of the cavity and the atoms on the transparency window. In addition, we discuss slow–fast light propagation phenomena. We demonstrate that, in relation to the magnomechanical coupling of YIG and the atom–cavity coupling strength, the group delay is dependent on the tunability of the optomechanical coupling strength.

The structure of the paper is as follows. In Section 2, we present the formula for the Hamiltonian and the appropriate quantum Langevin equations of the system under consideration and obtain the output field. In Section 3, we discuss MMIT and analyze the influence of the optomechanical coupling strength on the input spectrum. In Section 4, we demonstrate the essential conditions for the emergence of double Fano resonances in our hybrid system. In Section 5, we discuss the group delay for slow and fast light propagation. In Section 6, we study the feasibility of our system based on current experimental parameters and setups. We finish with our concluding remarks.

2. Model

2.1. Hamiltonian

In this subsection, we consider a hybrid cavity optomagnomechanical system,[37] composed of optical cavity photons, magnetostriction-induced vibration phonons, magnons in a YIG crystal and an ensemble of two-level atoms, as shown in Fig. 1(a). The magnomechanical displacement interacts with the optical cavity through radiation pressure, which is a type of dispersive interaction. This can be achieved by attaching a small, highly reflective mirror pad to the surface of a YIG microbridge.[57,58,60] The microscale YIG bridge is capable of supporting long-lived spin-wave excitations at gigahertz frequencies, along with mechanical vibration phonons ranging from tens to hundreds of megahertz.[60] The significant frequency difference between the magnon and mechanical modes allows for a dominant magnon–phonon dispersive coupling.[57] It is important that the attached mirror pad is fabricated to be much smaller than the YIG bridge to minimize bending displacement and ensure the bridge and mirror adhere closely, oscillating at nearly the same frequency. Alternatively, the "membrane-in-the-middle" configuration can be used,[61] where the YIG bridge is placed in the middle of the optical cavity, facilitating dispersive coupling between magnomechanical displacement and the optical cavity. The Hamiltonian of the system is given by[62]

$$\mathcal{H} = \mathcal{H}_{\rm free} + \mathcal{H}_{\rm int} + \mathcal{H}_{\rm drive}, \tag{1}$$

where the first part of the $\mathcal{H}$ is the free Hamiltonian terms

$$\mathcal{H}_{\rm free} = \hbar\left(\omega_c c^\dagger c + \omega_n n^\dagger n + \frac{\omega_a}{2}S_z + \frac{\omega_b}{2}\left(x^2+y^2\right)\right). \tag{2}$$

Here the first and second terms respectively describe the energy of the optical and magnon modes with c ($c^\dagger$) and n ($n^\dagger$) being the annihilation (creation) operators satisfying the usual commutation relation $[\mathcal{A},\mathcal{A}^\dagger]=1$, where $\mathcal{A}=c,n$. The parameters ω_c and ω_n denote the resonance frequencies of the cavity and magnon modes, respectively. It is worth noting that the value of frequency ω_n can be adjusted by altering the external bias magnetic field B, i.e., $\omega_n=\gamma B$ with $\gamma/2\pi = 28$ GHz·T^{-1}. The third term gives the energy of the atomic ensemble comprising N_a two-level atoms with natural frequency ω_a. S_+, S_- and S_z represent the spin operators of the atoms, defined as $S_{+,-,z}=\sum_i \sigma_{+,-,z}^{(i)}$, with σ_+, σ_- and σ_z being Pauli matrices, and satisfy the commutation relations $[S_+,S_-]=S_z$ and $[S_z,S_\pm]=\pm 2S_\pm$. The fourth term describes the energy of the mechanical vibration mode with x and y being respectively the position and momentum operator, such that $[x,y]=\mathrm{i}$. ω_b is the resonance frequency of the mechanical mode. The second part of $\mathcal{H}$ is the interaction Hamiltonian

$$\mathcal{H}_{\rm int} = \hbar\left(-g_c c^\dagger c x + g_n n^\dagger n x + g_a\left(S_+ c + S_- c^\dagger\right)\right). \tag{3}$$

Here the first term describes the interaction between the mechanical mode and the optical mode of rate g_c. The second term represents the interaction between the mechanical mode and the magnon mode of rate g_n. The last term corresponds to the interaction between the atomic mode and optical mode of rate $g_a=\rho\sqrt{\omega_c/(2\hbar\epsilon V)}$, with ρ as the atomic dipole moment, ϵ the vacuum permittivity and V the volume of the cavity. The last part of $\mathcal{H}$ is the driving Hamiltonian

$$\mathcal{H}_{\rm drive} = \mathrm{i}(c^+\epsilon_{\rm p}\,\mathrm{e}^{-\mathrm{i}\omega_{\rm p}t} - \mathrm{H.c}) + \mathrm{i}(\Omega_{\rm L} n^+\,\mathrm{e}^{-\mathrm{i}\omega_{\rm L}t} - \mathrm{H.c}), \tag{4}$$

where $\epsilon_{\rm p}=\sqrt{2\kappa_{\rm c}\mathcal{P}_{\rm p}/(\hbar\omega_{\rm p})}$ is the coupling strength between the cavity and the probe field. $\omega_{\rm p}$ ($\mathcal{P}_{\rm p}$) represents the frequency (power) of a probe field and $\kappa_{\rm c}$ is the decay rate of the cavity. The Rabi frequency $\Omega_{\rm L}=\frac{\sqrt{5}}{4}\gamma\sqrt{N}B_{\rm L}$ is the coupling strength between the magnon mode and the drive field with amplitude $B_{\rm L}$ and frequency $\omega_{\rm L}$. γ is the gyromagnetic ratio and N is the total number of spins in the YIG. If we assume that all atoms are initially in the ground state, so that

$S_z \simeq \langle S_z \rangle \simeq -N_a$, and the excitation probability of a single atom is small, we can define the dynamics of atomic polarization by bosonic annihilation operators $a = S_-/\sqrt{|\langle S_z \rangle|}$, and satisfy the commutation relation $[a, a^\dagger] = 1$. So, we obtain the total bosonized Hamiltonian, given by

$$\begin{aligned}\mathcal{H}/\hbar =\ & \omega_c c^\dagger c + \omega_n n^\dagger n + \omega_a a^\dagger a + \frac{\omega_b}{2}\left(x^2 + y^2\right) \\ & + g_N\left(a^\dagger c + a c^\dagger\right) - g_c c^\dagger c x + g_n n^\dagger n x \\ & + \mathrm{i}\left(\Omega_\mathrm{L} n^\dagger \mathrm{e}^{-\mathrm{i}\omega_\mathrm{L} t} - \mathrm{H.c}\right) + \mathrm{i}\left(c^\dagger \epsilon_\mathrm{p} \mathrm{e}^{-\mathrm{i}\omega_\mathrm{p} t} - \mathrm{H.c}\right), \quad (5)\end{aligned}$$

where $g_N = g_a\sqrt{N_a}$ is the effective atom–cavity coupling strength.

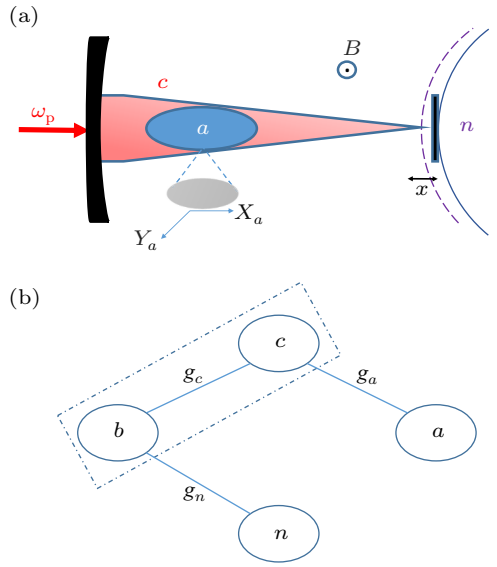


Fig. 1. (a) Schematic diagram of the atom-opto-magnomechanical system. Through the mediating effect of a mechanical vibration mode b induced by magnetostriction, the optical cavity mode c, driven by a probe field at frequency ω_p, couples to an ensemble of two-level atoms a and a magnon mode n in a YIG crystal. (b) The different coupling strengths in our system are as follows: g_c denotes the optomechanical coupling strength, g_n is the magnomechanical coupling strength and g_a is the atom–cavity coupling strength.

2.2. Quantum Langevin equations and the output field

The Heisenberg Langevin equations below can be used to characterize the system's quantum dynamics

$$\begin{aligned}\dot{c} &= -(\kappa_c + \mathrm{i}\Delta_c)c + \mathrm{i}g_c c x - \mathrm{i}g_N a + \epsilon_\mathrm{p}\mathrm{e}^{-\mathrm{i}\delta t} + \sqrt{2\kappa_c}c_\mathrm{in}, \\ \dot{a} &= -(\gamma_a + \mathrm{i}\Delta_a)a - \mathrm{i}g_N c + \sqrt{2\gamma_a}a_\mathrm{in}, \\ \dot{n} &= -(\kappa_n + \mathrm{i}\Delta_n)n - \mathrm{i}g_n n x + \Omega_\mathrm{L} + \sqrt{2\kappa_n}n_\mathrm{in}, \\ \dot{x} &= \omega_b y, \quad \dot{y} = -\omega_b x - \gamma_b y + g_c c^\dagger c - g_n n^\dagger n + \xi, \end{aligned} \quad (6)$$

where $\delta = \omega_\mathrm{p} - \omega_\mathrm{L}$, $\Delta_c = \omega_c - \omega_\mathrm{L}$, $\Delta_n = \omega_n - \omega_\mathrm{L}$ and $\Delta_a = \omega_a - \omega_\mathrm{L}$ are the detuning parameters. γ_b and κ_n are the dissipation rates of the mechanical and magnon modes, respectively. γ_a is the decay rate of the atoms. The terms $a_\mathrm{in}(t)$, $c_\mathrm{in}(t)$ and $n_\mathrm{in}(t)$ are the vacuum input noise operators, which have zero-mean values. $\xi(t)$ is the Hermitian Brownian noise operator acting on the mechanical oscillator.

The quantum Langevin equations (6) can be linearized by focusing on the steady-state values and only using first-order terms in the fluctuating operator: $\langle \mathcal{X} \rangle = \mathcal{X}_\mathrm{s} + \mathcal{X}_- \mathrm{e}^{-\mathrm{i}\delta t} + \mathcal{X}_+ \mathrm{e}^{\mathrm{i}\delta t}$, where $\mathcal{X} = c, a, n, x, y$. First, we examine the zero-order solutions, i.e., the steady-state solutions, represented as follows:

$$\begin{aligned} c_\mathrm{s} &= \frac{-\mathrm{i}g_N a_\mathrm{s}}{\kappa_c + \mathrm{i}\left(\Delta_c - g_c x_\mathrm{s}\right)} = \frac{-\mathrm{i}g_N a_\mathrm{s}}{\kappa_c + \mathrm{i}\bar{\Delta}_c}, \\ a_\mathrm{s} &= \frac{-\mathrm{i}g_N c_\mathrm{s}}{\gamma_a + \mathrm{i}\Delta_a}, \\ n_\mathrm{s} &= \frac{\Omega_\mathrm{L}}{\kappa_n + \mathrm{i}\left(\Delta_n + g_n x_\mathrm{s}\right)} = \frac{\Omega_\mathrm{L}}{\kappa_n + \mathrm{i}\bar{\Delta}_n}, \\ x_\mathrm{s} &= \frac{g_c |c_\mathrm{s}|^2 - g_n |n_\mathrm{s}|^2}{\omega_b}, \end{aligned} \quad (7)$$

where $\bar{\Delta}_c = \Delta_c - g_c x_\mathrm{s}$ and $\bar{\Delta}_n = \Delta_n + g_n x_\mathrm{s}$ are the effective detunings of the cavity and the magnon, respectively. We suppose that the coupling of the external microwave drive on magnon mode n is much stronger than the coupling of the external probe field ϵ_p. Under this assumption, the solution of the linearized quantum Langevin equations can be considered to be the first-order external probe field by ignoring all higher-order terms of ϵ_p. So, the solution for the cavity mode is given as

$$c_- = \epsilon_\mathrm{p}\left(h_3 + \frac{g_N^2}{h_1} - \mathcal{G}_c\frac{\mathcal{H}_6}{\mathcal{H}_5}\right)^{-1}, \quad (8)$$

where

$$\begin{aligned} & h_1 = \gamma_a + \mathrm{i}(\Delta_a - \delta), \quad h_2 = \gamma_a - \mathrm{i}(\Delta_a + \delta), \\ & h_3 = \kappa_c + \mathrm{i}(\bar{\Delta}_c - \delta), \quad h_4 = \kappa_c - \mathrm{i}(\bar{\Delta}_c + \delta), \\ & h_5 = \kappa_n + \mathrm{i}(\bar{\Delta}_n - \delta), \quad h_6 = \kappa_n - \mathrm{i}(\bar{\Delta}_n + \delta), \\ & h_7 = \omega_b^2 - \delta^2 - \mathrm{i}\gamma_b\delta, \quad \mathcal{H}_1 = 1 + \frac{g_N^2}{h_2 h_4}, \\ & \mathcal{H}_2 = \mathrm{i}h_7 - \omega_b\left(\frac{\mathcal{G}_c^2}{\mathcal{H}_1 h_4} + \frac{\mathcal{G}_n^2}{h_6}\right), \quad \mathcal{H}_3 = \omega_b\frac{-\mathcal{G}_n^2}{h_5} - \mathrm{i}h_7, \\ & \mathcal{H}_4 = \omega_b\left(\frac{\mathcal{G}_c^2}{h_4\mathcal{H}_1} + \frac{\mathcal{G}_n^2}{h_6}\right), \quad \mathcal{H}_5 = \mathcal{H}_3 - \frac{\omega_b\mathcal{G}_n^2\mathcal{H}_4}{h_5\mathcal{H}_2}, \\ & \mathcal{H}_6 = \omega_b\mathcal{G}_c\left(1 + \frac{\mathcal{H}_4}{\mathcal{H}_2}\right). \end{aligned}$$

Here, $\mathcal{G}_c = G_c/\sqrt{2}$ and $\mathcal{G}_n = G_n/\sqrt{2}$, with $G_c = \mathrm{i}\sqrt{2}g_c c_\mathrm{s}$ and $G_n = \mathrm{i}\sqrt{2}g_n n_\mathrm{s}$ being the effective opto- and magnomechanical coupling strengths. It should be noted that the solution for the cavity in Eq. (8) is derived under the condition that $|\Delta_a|, |\tilde{\Delta}_c|, |\tilde{\Delta}_n| \gg \gamma_a, \kappa_c, \kappa_n$. We use the input–output standard relation $\epsilon_\mathrm{out} = \epsilon_\mathrm{in} - 2\kappa_c\langle c \rangle$,[63] where ϵ_in (ϵ_out) is the input field (output field) vector, and the amplitude of the output field can be written as

$$\epsilon_\mathrm{out} = \frac{2\kappa_c c_-}{\epsilon_\mathrm{p}} = \epsilon_\mathrm{R} + \mathrm{i}\epsilon_\mathrm{I}, \quad (9)$$

where $\epsilon_{\rm R}$ is the real part of $\epsilon_{\rm out}$, which describes the absorption spectrum of the output probe field frequency. $\epsilon_{\rm I}$ is the imaginary part of $\epsilon_{\rm out}$, which describes the dispersion spectrum of the probe field frequency.

3. Magnomechanically induced transparency

In this section we will study the MMIT in the system under consideration and investigate the impact of the decay rates of the cavity and the atomic ensemble on the transparency window. The parameters we use were obtained in a recent experiment on a hybrid magnomechanical system:[37,38,59] $\omega_n/2\pi =$ 10 GHz, $\omega_b/2\pi = 40$ MHz, $\lambda_{\rm p} = 852$ nm, $\kappa_n/2\pi = 1$ MHz, $\gamma_a = \kappa_n$, $\kappa_c = 2\kappa_n$, $\gamma_b/2\pi = 10^2$ Hz, $g_N/2\pi = 8$ MHz and $\bar{\Delta}_n = \omega_b$. The strong optomechanical coupling $G_c/2\pi =$ 8 MHz can be achieved with a laser power $\mathcal{P}_{\rm p} \simeq 5.5$ mW for $g_c/2\pi = 1$ kHz at detunings $\bar{\Delta}_c \simeq 0.5\omega_b$ and $\Delta_a = -\omega_b$. According to Eq. (9), the rescaled transmission field associated with the probe field can be written as follows:

$$\mathcal{T} = \frac{\epsilon_{\rm p} - 2\kappa_c c_-}{\epsilon_{\rm p}}. \tag{10}$$

The definition of the phase ϕ for the transmitted probe field $\mathcal{T}$ is as follows:[64]

$$\phi = {\rm Arg}[\mathcal{T}]. \tag{11}$$

We plot in Fig. 2(a), the transmission $|\mathcal{T}|^2$ spectrum of the probe field versus the normalized probe frequency δ/ω_b for various values of the effective optomechanical coupling G_c. From the black line in Fig. 2(a) one can easily observe that there are no signatures of MMIT in the transmission spectrum of the probe field when the optical mode is not coupled with the mechanical mode ($G_c = 0$). Moreover, in the red line, the double MMIT window appears in the output probe field due to the effective optomechanical coupling $G_c/2\pi = 4$ MHz. In comparing the green, blue and red lines in Fig. 2(a), the transparency windows become wider and deeper with increasing values of the effective optomechanical coupling G_c. These results clearly prove the existence of a double MMIT window in the output probe field when the cavity optical mode is only coupled to the mechanical mode (phonon). This physical phenomenon is very similar to both OMIT and EIT.[65,66]

In Fig. 2(b), we plot the phase ϕ of the transmitted probe field $\mathcal{T}$ versus the normalized probe detuning δ/ω_b of the probe field for various values of G_c. We find when the effective optomechanical coupling strength is absent ($G_c = 0$), no transparency window appears in the phase spectra of the transmitted probe field. On the other hand, two MMIT windows appear in the output probe field because the optical mode of the system is now coupled to the mechanical mode ($G_c/2\pi = 4$ MHz). As the effective optomechanical coupling G_c increases, the transparency window becomes wider.

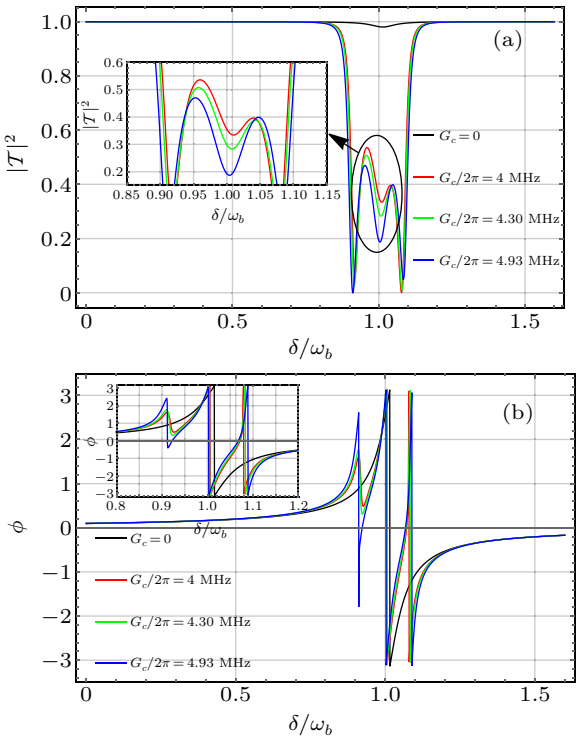


Fig. 2. Plot of the transmission $|\mathcal{T}|^2$ and the phase ϕ as a function of δ/ω_b for different values of the optomechanical coupling strength G_c with $G_n/2\pi = 5.6$ MHz. For other parameters, refer to the text.

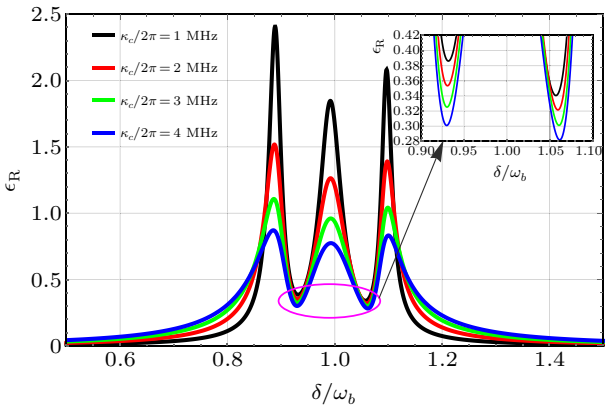


Fig. 3. Plot of the absorption $\epsilon_{\rm R}$ as a function of normalized probe frequency δ/ω_b for different values of the decay rate of the cavity with $G_c/2\pi = 6$ MHz and $G_n/2\pi = 6$ MHz. For other parameters, refer to the text.

In Fig. 3 we plot the real part $\epsilon_{\rm R}$ of the output field versus the normalized probe detuning δ/ω_b of the probe field for various values of the decay rate of the cavity when the value of the effective optomechanical coupling strength is fixed. It can be observed that the sideband absorption peaks decrease as the cavity delay rate increases. Additionally, we note that as the decay rate increases the transparency window becomes wider and deeper.

In Fig. 4 we display the absorption $\epsilon_{\rm R}$ versus the normalized probe detuning δ/ω_b for various values of the decay rate of the atomic ensemble, while keeping the optomechanical coupling strength G_c fixed. We note that increasing the decay rate γ_a leads to an increase in the peak of the double windows, which is consistent with the findings in previous work.[67]

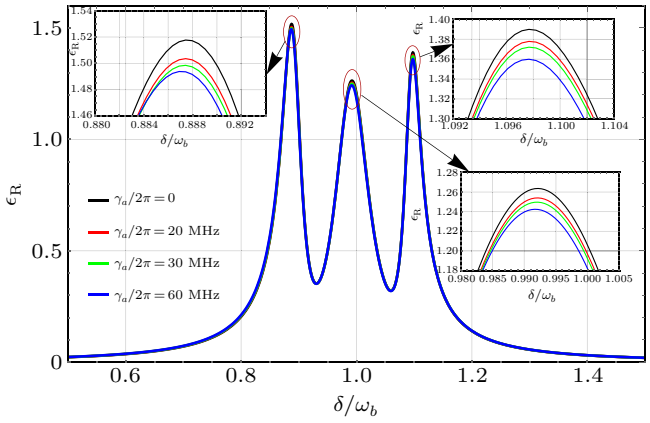


Fig. 4. Plot of the absorption ϵ_R as a function of δ/ω_b for different values of the decay rate of the atomic ensemble with $G_c/2\pi = 6$ MHz and $G_n/2\pi = 5.6$ MHz. For other parameters, refer to the text.

4. Fano resonances

In this section, we will discuss the appearance of Fano line shapes in the output spectrum along with their underlying physical mechanism. Unlike the symmetric resonance curves observed in phenomena such as EIT, OMIT and MMIT windows, the Fano resonance is characterized by a distinctly asymmetric shape.[31,33] Fano resonances have been detected in systems previously exhibiting EIT by carefully adjusting system parameters.[31,33,37,68–70] The unique asymmetric profile of Fano resonances in systems with optomechanical-like interactions is attributed to non-resonant interactions. For example, within a conventional optomechanical framework, the emergence of asymmetric Fano resonance shapes in the spectral distribution can occur when the anti-Stokes process does not match the resonant frequency of the cavity.[33,69]

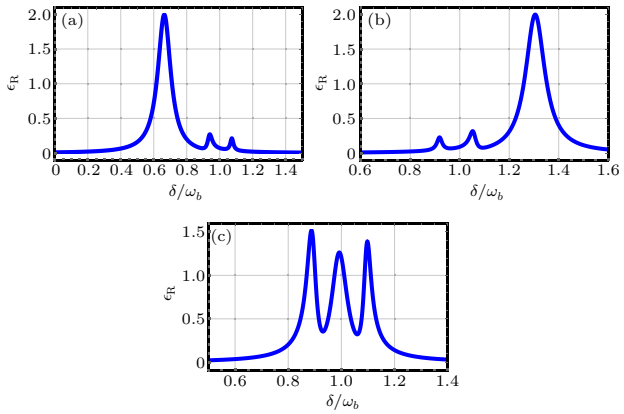


Fig. 5. Fano lineshapes in the asymmetric absorption ϵ_R profiles are shown versus the normalized probe frequency δ/ω_b with $G_c/2\pi = 6$ MHz and $G_n/2\pi = 5.6$ MHz: (a) $\bar{\Delta}_c = 0.2\omega_b$, (b) $\bar{\Delta}_c = 0.8\omega_b$ and (c) $\bar{\Delta}_c = 0.5\omega_b$. The other parameters are given in Section 3.

Asymmetric Fano shapes can be seen in Figs. 5(a) and 5(b) for various non-resonant cases, where the real part of the output field ϵ_R is plotted against the normalized detuning δ/ω_b. In Fig. 5(a), with the phonon–photon coupling set to $G_c/2\pi = 6$ MHz, the output spectrum exhibits an asymmetric window profile due to the presence of a non-resonant process ($\bar{\Delta}_c = 0.2\omega_b$). Furthermore, we set the effective detuning value $\bar{\Delta}_c$ of the driving field and phonon mode to $0.8\omega_b$. As shown in Fig. 5(b), the double Fano resonance peak shifts from the right ($\bar{\Delta}_c = 0.2\omega_b$) to the left ($\bar{\Delta}_c = 0.8\omega_b$). In Fig. 5(c), the Fano resonance disappears when we consider the resonant case $\bar{\Delta}_c = 0.5\omega_b$.

5. The group delay

In this section we study the group delay of the output signal as a function of the normalized detuning δ/ω_b for various values of phonon–photon coupling strength G_c.

The phase of the transmitted probe field in Eq. (11) is related to the group delay τ of the output field by the following relation:[64,71]

$$\tau = \frac{\partial\phi}{\partial\omega_p} = \mathrm{Im}\left[\frac{1}{\mathcal{T}}\frac{\partial\mathcal{T}}{\partial\omega_p}\right]. \tag{12}$$

This implies that larger group delays result from quicker phase dispersion and vice versa. Additionally, a negative phase slope indicates a negative group delay $\tau < 0$, corresponding to fast light propagation, while a positive phase slope means a positive group delay $\tau > 0$, corresponding to slow light propagation.

In Fig. 6, we plot the group delay of the output field at the probe field frequency versus the normalized probe frequency δ/ω_b for various values of the optomechanical coupling strength G_c. In Fig. 6(a) we note that for $G_c/2\pi = 4$ MHz a negative group delay of the output field is achieved at $\delta \approx 0.91\omega_b$, which corresponds to the fast light effect of the output probe field. In contrast, a positive group delay, i.e., the slow light effect of the output probe field, is achieved at $\delta \approx 1.07\omega_b$. Moreover, by increasing the effective optomechanical coupling G_c, the fast light increased around $\delta \approx 0.91\omega_b$, and at $\delta \approx 1.07\omega_b$ the slow light decreased, as depicted in Figs. 6(b) and 6(c). Furthermore, we observe that for $G_c/2\pi = 4.93$ MHz, the slow light enhances at $\delta \approx 0.91\omega_b$ and the group delay τ of the output field reaches $\tau \approx 97.60$ μs, as depicted in Fig. 6(d). By comparing the evolution of transmission in Fig. 2(a) with Fig. 6 for $G_c/2\pi = 4$ MHz it is observed that the peak ($\tau > 0$) occurs at $\omega_p - \omega_L \simeq 1.07\omega_b$, where the transmission is converted from absorption to transmission. This peak can be explained by sudden increases of the phase ϕ at $\omega_p - \omega_L \simeq 1.07\omega_b$ (see Eq. (12)), as depicted in Fig. 2(b). The physical explanation for the group delay is the tunability of the quantum interference between the probe field and the anti-Stokes field. This implies that the group delay can be dynamically tuned to modulate fast and slow light by manipulating the strength of the optomechanical coupling.

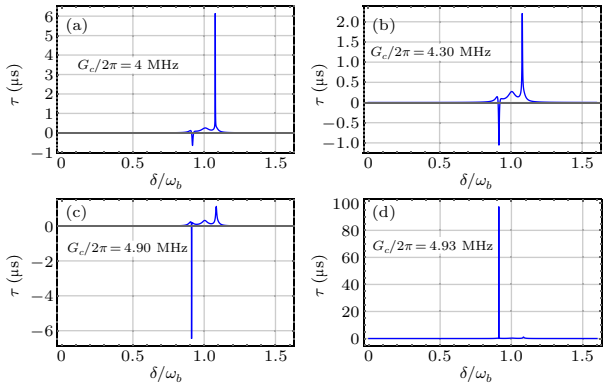


Fig. 6. The group delay τ of the transmitted probe field as a function of the normalized probe frequency δ/ω_b for different values of the coupling strength G_c with $G_n/2\pi = 5.6$ MHz: (a) $G_c/2\pi = 4$ MHz, (b) $G_c/2\pi = 4.30$ MHz, (c) $G_c/2\pi = 4.90$ MHz, (d) $G_c/2\pi = 4.93$ MHz. See text for the other parameters.

6. Feasibility

Here, we evaluate the experimental feasibility of our system based on the current experiments. Our system comprises two interconnected subsystems: a magnomechanical subsystem and an optomechanical subsystem. A recent experiment demonstrated the interaction between a highly polished single-crystal YIG sphere and a three-dimensional microwave cavity.[37] Moreover, we have analyzed the parametric regime, which is applicable only when the magnon population is substantially lower than the total spin of the system. Specifically, this condition requires that the average magnon number, $\langle n^\dagger n\rangle$, is much less than $5N$, the total spin of the Fe^{3+} ions in YIG (where $s = 5/2$).[37] While the magnomechanical component has been demonstrated in previous studies, the optomechanical aspect has been experimentally realized.[72] Experimental studies on atom trapping have revealed that ground and excited atoms, when positioned appropriately, are unaffected by external magnetic fields. This phenomenon is described in Ref. [73]. In this work, we have utilized the parameters used in Ref. [62]. Consequently, the proposed system, which utilizes a high-quality YIG sphere and an atomic ensemble within an opto-magnomechanical cavity, appears to be experimentally feasible.

7. Conclusion

In conclusion, we have investigated the MMIT, Fano resonance and slow–fast light in an atom-opto-magnomechanical system. We have discussed the transmission and the phase spectra of a weak probe field under a strong control field. Due to the presence of photon–phonon interactions we have observed OMIT, and the phonon–magnon interactions lead to MMIT. We have shown the absence of MMIT as a result of the absence of photon–phonon coupling. We have found two MMIT windows in the output probe spectra due to the presence of photon–phonon and magnon–photon interactions. We have studied the influence of decay rate of the cavity and the atomic ensemble on the MMIT windows. Furthermore, we have discussed in detail the phenomenon of Fano resonance caused by the presence of anti-Stokes processes in the system. We investigated slow and fast light propagation conditions that can be modulated by various system parameters. It was shown that, in an opto-magnomechanical system, the group delay is enhanced by adjusting phonon–photon coupling strength.

Acknowledgment

M. Amghar acknowledges the financial support of the National Center for Scientific and Technical Research (CNRST) through the 'PhD-Associate Scholarship-PASS' program.

References

[1] Agarwal G S and Huang S 2010 *Phys. Rev. A* **81** 041803
[2] Liao Q, Xiao X, Nie W and Zhou N 2020 *Opt. Express* **28** 5288
[3] Safavi-Naeini A H, Alegre T M, Chan J, Eichenfield M, Winger M, Lin Q and Painter O 2011 *Nature* **472** 69
[4] Weis S, Rivière R, Deléglise S, Gavartin E, Arcizet O, Schliesser A and Kippenberg T J 2010 *Science* **330** 1520
[5] Amghar M and Amazioug M 2024 *Int. J. Quantum Inf.* 2450043
[6] Qasymeh M, Hunza M, Asjad M, Abbas T, Teklu B and Eleuch H *Tunable Electromagnetically Induced Multi-Transparencies in Hybrid Optomechanical System Incorporating Atomic Medium* Available at SSRN 4210409
[7] Zhang X Y, Zhou Y H, Guo Y Q and Yi X X 2018 *Phys. Rev. A* **98** 033832
[8] Lei F C, Gao M, Du C, Jing Q L and Long G L 2015 *Opt. Express* **23** 11508
[9] Boller K J, Imamoğlu A and Harris S E 1991 *Phys. Rev. Lett.* **66** 2593
[10] Fleischhauer M, Imamoglu A and Marangos J P 2005 *Rev. Mod. Phys.* **77** 633
[11] Paspalakis E and Knight P L 2002 *Phys. Rev. A* **66** 015802
[12] Wu Y and Yang X 2005 *Phys. Rev. A* **71** 053806
[13] Roghani M, Breuer H P and Helm H 2010 *Phys. Rev. A* **81** 033418
[14] Abdumalikov Jr A A, Astafiev O, Zagoskin A M, Pashkin Y A, Nakamura Y and Tsai J S 2010 *Phys. Rev. Lett.* **104** 193601
[15] Abdi M, Pirandola S, Tombesi P and Vitali D 2012 *Phys. Rev. Lett.* **109** 143601
[16] Asjad M, Li J, Zhu S Y and You J Q 2023 *Fundam. Res.* **3** 3
[17] Singh S K, Mazaheri M, Peng J X, Sohail A, Gu Z and Asjad M 2023 *Quant. Inf. Process.* **22** 198
[18] Amazioug M and Nassik M 2019 *Int. J. Quantum Inf.* **17** 1950045
[19] Amazioug M, Singh S, Teklu B and Asjad M 2023 *Entropy* **25** 1462
[20] Amazioug M and Daoud M 2021 *Eur. Phys. J. D* **75** 178
[21] Amazioug M, Teklu B and Asjad M 2023 *Sci. Rep.* **13** 3833
[22] Liao J Q, Wu Q Q and Nori F 2014 *Phys. Rev. A* **89** 014302
[23] Amazioug M, Dutykh D S and Asjad M 2023 arXiv:2311.06578v3 [quant-ph]
[24] Noura C, M'bark A and Mohamed A 2024 *Phys. Lett. A* **519** 129712
[25] Marangos J P 1998 *J. Mod. Opt.* **45** 471
[26] Jiang C, Liu H, Cui Y, Li X, Chen G and Chen B 2013 *Opt. Express* **21** 12165
[27] Wu S C, Qin L G, Jing J, Yan T M, Lu J and Wang Z Y 2018 *Phys. Rev. A* **98** 013807
[28] Han Y, Cheng J and Zhou L 2011 *J. Phys. B: At. Mol. Opt. Phys.* **44** 165505
[29] Li X, Nie W, Chen A and Lan Y 2018 *Phys. Rev. A* **98** 053848
[30] Jiang C, Jiang L, Yu H, Cui Y, Li X and Chen G 2017 *Phys. Rev. A* **96** 053821
[31] Fano U 1961 *Phys. Rev.* **124** 1866
[32] Zangeneh-Nejad F and Fleury R 2019 *Phys. Rev. Lett.* **122** 014301
[33] Qu K and Agarwal G S 2013 *Phys. Rev. A* **87** 063813
[34] Rybin M V, Khanikaev A B, Inoue M, Samusev K B, Steel M J, Yushin G and Limonov M F 2009 *Phys. Rev. Lett.* **103** 023901

[35] Xiao Y F, Li M, Liu Y C, Li Y, Sun X and Gong Q 2010 *Phys. Rev. A* **82** 065804
[36] Amghar M, Chabar N and Amazioug M 2024 arXiv:2407.04430v1 [quant-ph]
[37] Zhang X, Zou C L, Jiang L and Tang H X 2016 *Sci. Adv.* **2** e1501286
[38] Li J, Zhu S Y and Agarwal G S 2018 *Phys. Rev. Lett.* **121** 203601
[39] Potts C A, Varga E, Bittencourt V A, Kusminskiy S V and Davis J P 2021 *Phys. Rev. X* **11** 031053
[40] Shen R C, Li J, Fan Z Y, Wang Y P and You J Q 2022 *Phys. Rev. Lett.* **129** 123601
[41] Li J, Zhu S Y and Agarwal G S 2019 *Phys. Rev. A* **99** 021801
[42] Li J and Zhu S Y 2019 *New J. Phys.* **21** 085001
[43] Ding M S, Zheng L and Li C 2020 *JOSA B* **37** 627
[44] Lachance-Quirion D, Tabuchi Y, Gloppe A, Usami K and Nakamura Y 2019 *Appl. Phys. Express* **12** 070101
[45] Kong C, Wang B, Liu Z X, Xiong H and Wu Y 2019 *Opt. Express* **27** 5544
[46] Yuan H Y, Cao Y, Kamra A, Duine R A and Yan P 2022 *Phys. Rep.* **965** 1
[47] Ding M S, Zheng L and Li C 2019 *Sci. Rep.* **9** 15723
[48] Yu M, Shen H and Li J 2020 *Phys. Rev. Lett.* **124** 213604
[49] Sarma B, Busch T and Twamley J 2021 *New J. Phys.* **23** 043041
[50] Xiong H 2023 *Fundam. Res.* **3** 8
[51] Xie J K, Ma S L and Li F L 2020 *Phys. Rev. A* **101** 042331
[52] Ren Y L, Ma S L, Xie J K, Li X K, Cao M T and Li F L 2022 *Phys. Rev. A* **105** 013711
[53] Ren Y L, Ma S L and Li F L 2022 *Phys. Rev. A* **106** 053714
[54] Xie J, Ma S, Ren Y, Li X, Gao S and Li F 2023 *New J. Phys.* **25** 073009
[55] Ren Y L, Ma S L, Xie J K, Li X K and Li F L 2021 *Opt. Express* **29** 41399
[56] Fan Z Y, Shen R C, Wang Y P, Li J and You J Q 2022 *Phys. Rev. A* **105** 033507
[57] Fan Z Y, Qian H and Li J 2022 *Quant. Sci. Technol.* **8** 015014
[58] Fan Z Y, Qiu L, Gröblacher S and Li J 2023 *Laser Photonics Rev.* **17** 2200866
[59] Liao Q, Peng K and Qiu H 2023 *Chin. Phys. B* **32** 054205
[60] Heyroth F, Hauser C, Trempler P, Geyer P, Syrowatka F, Dreyer R, Ebbinghaus S G, Woltersdorf G and Schmidt G 2019 *Phys. Rev. Appl.* **12** 054031
[61] Thompson J D, Zwickl B M, Jayich A M, Marquardt F, Girvin S M and Harris J G E 2008 *Nature* **452** 72
[62] Fan Z Y, Qian H, Zuo X and Li J 2023 *Phys. Rev. A* **108** 023501
[63] Gardiner C and Zoller P 2004 *Quantum noise: a handbook of Markovian and non-Markovian quantum stochastic methods with applications to quantum optics* (Springer Science and Business Media)
[64] Tarhan D, Huang S and Müstecaplıoğlu Ö E 2013 *Phys. Rev. A* **87** 013824
[65] Akram M J, Khan M M and Saif F 2015 *Phys. Rev. A* **92** 023846
[66] Akram M J, Ghafoor F and Saif F 2015 *J. Phys. B: At. Mol. Opt. Phys.* **48** 065502
[67] Liao Q, Peng K and Qiu H 2023 *Chin. Phys. B* **32** 054205
[68] Yasir K A and Liu W M 2016 *Sci. Rep.* **6** 22651
[69] Ullah K 2019 *Eur. Phys. J. D* **73** 267
[70] Jiang C, Jiang L, Yu H, Cui Y, Li X and Chen G 2017 *Phys. Rev. A* **96** 053821
[71] Gu K H, Yan X B, Zhang Y, Fu C B, Liu Y M, Wang X and Wu J H 2015 *Opt. Commun.* **338** 569
[72] Safavi-Naeini A H *et al.* 2011 *Nature* **472** 69
[73] Raab E L, Prentiss M, Cable A, Chu S and Pritchard D E 1987 *Phys. Rev. Lett.* **59** 2631